

## GEOPHYSICS

# Slab2, a comprehensive subduction zone geometry model

Gavin P. Hayes<sup>1\*</sup>, Ginevra L. Moore<sup>1,2†</sup>, Daniel E. Portner<sup>1,3</sup>, Mike Hearne<sup>1</sup>, Hanna Flamme<sup>1,2‡</sup>, Maria Furtney<sup>1§</sup>, Gregory M. Smoczyk<sup>1</sup>

Subduction zones are home to the most seismically active faults on the planet. The shallow megathrust interfaces of subduction zones host Earth's largest earthquakes and are likely the only faults capable of magnitude 9+ ruptures. Despite these facts, our knowledge of subduction zone geometry—which likely plays a key role in determining the spatial extent and ultimately the size of subduction zone earthquakes—is incomplete. We calculated the three-dimensional geometries of all seismically active global subduction zones. The resulting model, called Slab2, provides a uniform geometrical analysis of all currently subducting slabs.

**S**ubduction zones account for about ~90% of the energy released by historical earthquakes globally. The world's largest earthquakes occur there, and often such events are both damaging and deadly. Knowledge of the geometry of subducting slabs is important to the understanding of earthquake and tsunami hazards associated with subduction zones. Slab1.0 (1), the predecessor to the model presented here, was introduced as a three-dimensional (3D) model of the geometries of subduction zones worldwide that synthesized results from global earthquake monitoring and regional seismotectonic studies

and provided data at a resolution useful for seismic and tsunami hazard studies. Many authors have used Slab1.0 as a reference for earthquake source characterization (2, 3). The geometries provided by the model have been important for global earthquake hazard analysis (4). The model has also been used in studies of geophysical processes, such as megathrust behavior (5, 6), slow slip (7), seismic anisotropy (8), volcano petrology (9), tsunami hazard (10), and mantle flow (11). However, some aspects of Slab1.0 are now out of date with respect to current knowledge of subduction zone structure. Moreover, the approaches

used in Slab1.0 proved inadequate for some important subduction zones, such as those in the Himalaya, eastern Indonesia, Manila, and New Zealand. Though several other global subduction zone geometry databases exist, most are limited in either spatial extent or resolution (12, 13) (fig. S1), particularly at shallow depths (<50 km), where the largest, most hazardous subduction zone earthquakes (“megathrust” events) occur and where most tsunamigenic earthquakes are located. As tsunamis are very sensitive to the geometry of the fault on which slip occurred, detailed knowledge of the shape of the megathrust is critical for hazard assessment.

Here, we present Slab2, a new model describing the 3D geometries of all seismically active subduction zones worldwide (Fig. 1). We model slabs from the near-surface (oceanic trenches for most slabs) to their deepest expressions in the upper mantle. In all, Slab2 describes the detailed geometry of more than 24 million square kilometers of subducted slabs. We made a variety of enhancements to Slab2 that set it apart from Slab1.0 and other global subduction zone models. First and foremost, we collected more data that image subducting slabs. Data sources come from

<sup>1</sup>U.S. Geological Survey National Earthquake Information Center, Golden, CO, USA. <sup>2</sup>Department of Geophysics, Colorado School of Mines, Golden, CO, USA. <sup>3</sup>Department of Geosciences, University of Arizona, Tucson, AZ, USA.

\*Corresponding author. Email: ghayes@usgs.gov †Present address: School of Oceanography, University of Washington, Seattle, WA, USA. ‡Present address: Chevron, Houston, TX, USA.

§Present address: Department of Earth, Environmental and Planetary Sciences, Rice University, Houston, TX, USA.

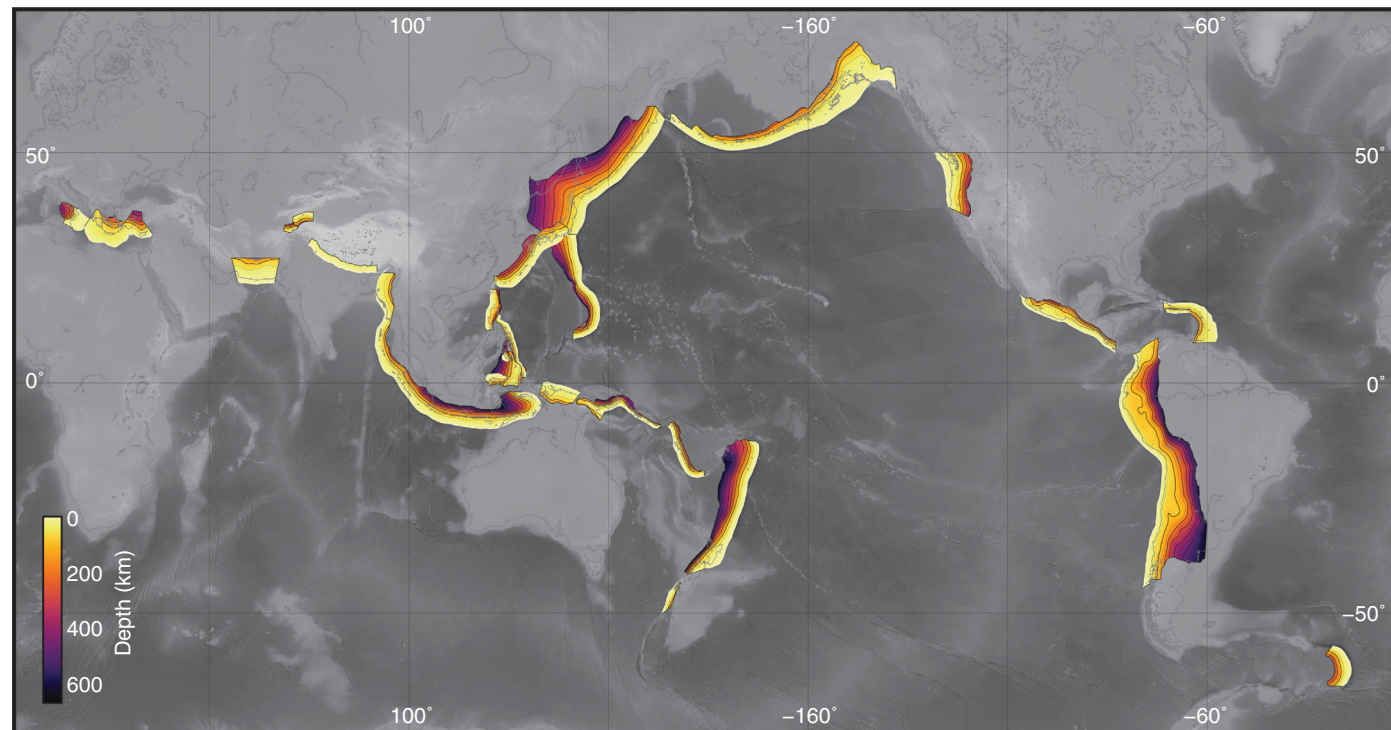


**Fig. 1. The global distribution of models included in Slab2.** Models are colored by depth. Slab2 and the code base used to create it are openly available via ScienceBase (31).

an improved density of active-source seismic data interpretations, receiver functions, local and regional seismicity catalogs (from both regional networks and relocation studies), and seismic tomography models (14) (fig. S2). Our inclusion of these data facilitates a much more complete imaging of slab surfaces than is possible with global earthquake and moment tensor catalogs alone. Second, we have substantially modified our slab depth modeling approach. Rather than using the 2D-to-3D iterative process of Slab1.0, we moved straight to modeling the 3D structure of the slab. We first modeled the slab depth at individual nodes over a grid for each subduction zone (15) and then interpolated those depths onto a 3D grid, or surface.

Our approach (15) (figs. S3 to S5) allowed us to model all known active subduction zones globally, creating a complete collection of subduction zone geometry models, built routinely and via the same modeling approach (Table 1 and table S3). With Slab2, we improved how overturned slabs (e.g., the Izu-Bonin slab) are handled (fig. S6) by generating such slab surfaces in a rotated, strike-parallel reference frame. Slab2 includes models for sparsely seismic yet very hazardous subduction zones such as the Himalaya, Manila, Cotabato, Sulawesi, and northern New Guinea. Slab2 models the little-studied subduction zone geometries of the Halmahera and Papua New Guinea slabs, which both contain sections with inverted U-shaped structure (Figs. 2 and 3). In the Philippines region (Fig. 2), at least four subducting slabs overlap one another, creating a complex mosaic of subducting slabs in which the shallow Philippine Sea, Cotabato, and Sulawesi slabs are underlain by the large, buried, and inverted U-shaped Halmahera slab. Although the shape of the latter slab has been previously studied [e.g., (16) and (17)], the detailed interaction with surrounding slabs, including the smaller Cotabato and Sulawesi subduction zones, is poorly understood. Each of these slabs has hosted large to great-sized earthquakes in the past, and improved understanding of their geometries is critical for hazard analyses of the surrounding, highly populated region. Similarly, beneath Papua New Guinea, the Solomon Sea slab has subducted to the south and north (Fig. 3), as first observed by Ripper (18) and modeled more recently by Holm and Richards (19). Given the clear connectivity between the southern and northern limbs of this subduction zone seen in our geometry model and given that active subduction continues to the north, substantial tectonic complexity is implied in the transition region between the northward-subducting New Britain slab and the connected but buried arm of the slab farther west (Fig. 3).

Elsewhere, the addition of datasets improves how flat slab regions are defined. For example, in Central America, Slab1.0 failed to accurately capture the flat slab beneath southern Mexico because of its lack of seismicity. Additional receiver function datasets (20) allow Slab2 to better model the extent of the flat slab. This region is near the location of the destructive 19 September 2017 earthquake (21) (fig. S7). In South America,

tomographic datasets (22) enable Slab2 to resolve the full extent of the flat slab beneath southern Peru (fig. S8) and the aseismic deep slab beneath southern Chile. In the Cascadia region, tomographic data extend our image of the subducting slab well beyond the depth extent of previous models (e.g., Slab1.0) (23). In all cases, the expanded data coverage and improved methodology of Slab2 facilitate a more complete definition of subduction zone geometry than was possible with the model's predecessor, Slab1.0.

Inherent to our modeling approach is the creation of a filtered, slab-related catalog of seismicity for each subduction zone. Among other applications, these catalogs can be used to improve estimates of properties of the seismogenic zone (1, 24), commonly used for seismic hazard analyses. We define the shallow and deep limits of the seismogenic zone as the 10th and 90th percentiles of a double-normal distribution fit to the number of thrust earthquakes in our filtered dataset for each subduction zone. We modeled

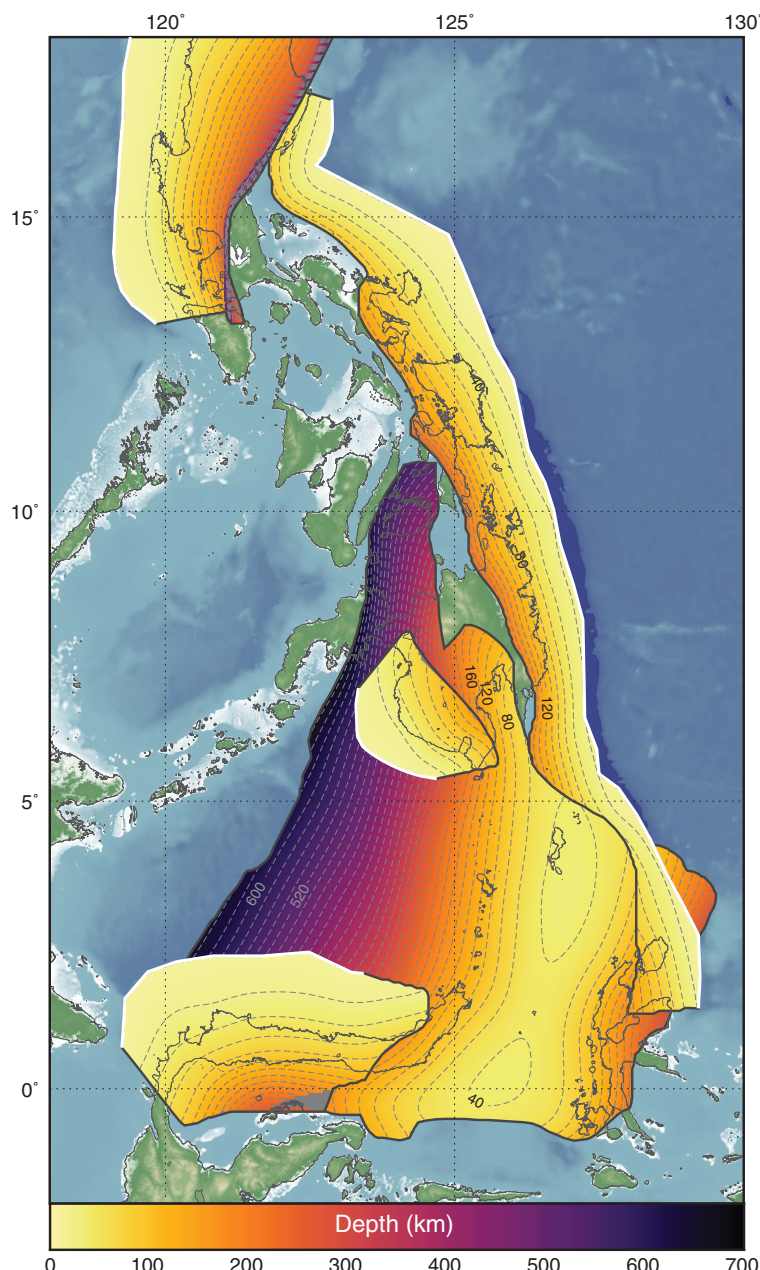


**Fig. 2. Slab2 models in the region surrounding the Philippines.** Here, five slabs (the Manila, Philippine, Cotabato, Halmahera, and Sulawesi slabs, from north to south) interact with one another. The Halmahera slab is an inverted U-shaped subduction zone that is completely buried and has no surface expression. It underlies the Cotabato and Sulawesi slabs on its western limb and abuts or underlies the Philippine slab on its eastern limb.

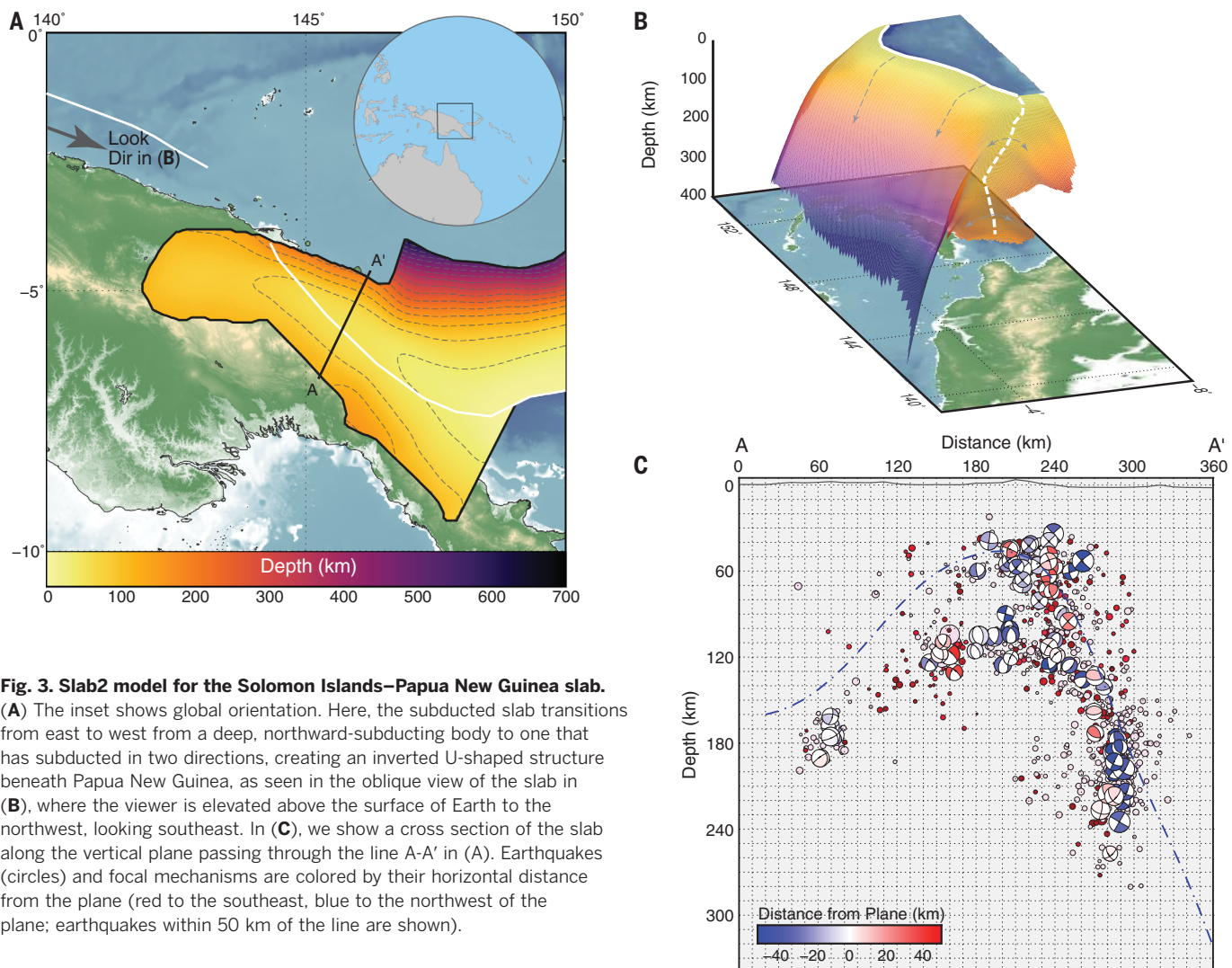


**Table 1. A selection of subduction zone models included in Slab2.** Shallow (Ss) and deep (Sd) seismogenic zone limits and corresponding seismogenic zone widths (Sw) are shown. See table S3 for expanded content.  $\delta$ ,  $\Phi$ , and  $\lambda$  represent the average subduction zone interface dip, strike, and rake, respectively, in the seismogenic zone.  $n$ , number of contributing earthquakes;  $M_{\max}$ , maximum historically observed magnitude for each subduction zone.

Model no.	Subduction zone arc	Slab2 code	$n$	Ss (km)	Sd (km)	Sw (km)	$\delta$ ( $^{\circ}$ )	$\Phi$ ( $^{\circ}$ )	$\lambda$ ( $^{\circ}$ )	$M_{\max}$
1	Aleutians	alu	470	12	45	124	14	265	124	9.2
3	Central America	cam*	701	11	42	91	20	301	86	8.1
11	Izu-Bonin	izu	218	10	37	96	15	174	93	7.5
12	Kermadec	ker	707	10	47	129	16	205	93	8.3
13	Kuril	kur	1162	13	54	138	15	227	89	9.1
15	Manila	man	90	14	48	69	29	130	89	7.2
18	New Guinea	png	81	10	41	191	9	106	89	8.2
19	Philippines	phi	121	11	49	79	28	142	76	7.8
21	Ryukyu	ryu	265	13	47	111	17	236	99	8.8
22	South America	sam	1370	11	45	118	15	356	85	9.5
23	Scotia	sco	70	11	46	87	17	175	109	7.5
24	Solomon Islands	sol	627	12	53	77	33	287	96	8.0
26	Sumatra/Java	sum	706	11	53	153	17	281	100	9.1
27	Vanuatu	van	467	11	49	75	29	322	90	8.0

\*In Slab1.0, this model was named "mex."

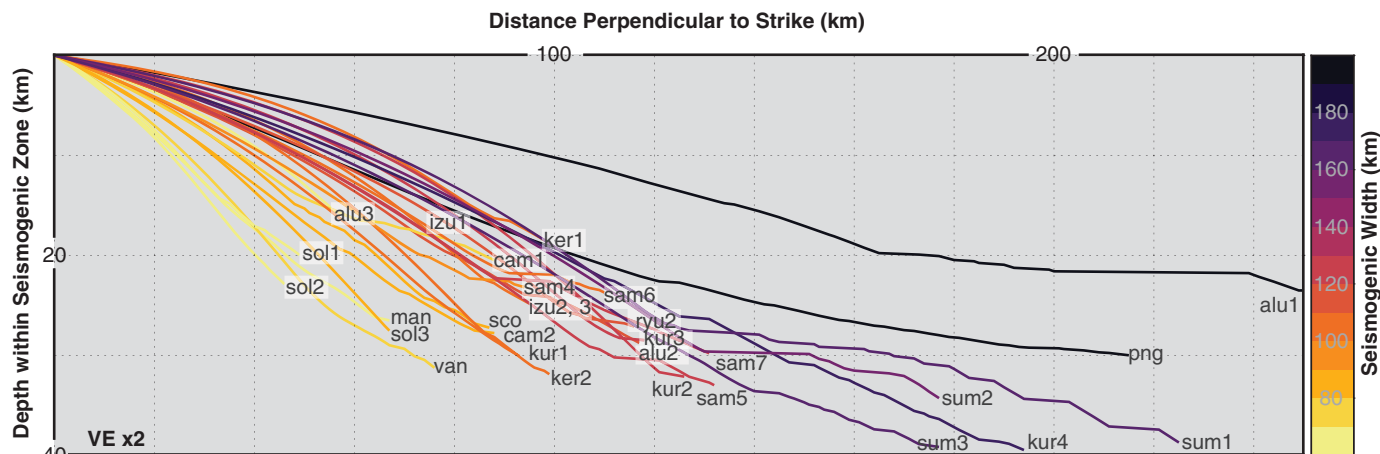


**Fig. 4. The shape of the seismogenic zone in global subduction zones.** Zones are color coded by the Sw. Line labels are defined in Table 1. The figure has a vertical exaggeration of 2 (VE ×2).

seismogenic zone width (Sw) (the length of the seismogenic zone along the dip direction of the slab) only for those slabs having more than 50 identifiable thrust-type earthquakes in our filtered datasets used to constrain slab depth (Fig. 4). The deep limit of the seismogenic zone varies globally from ~37 km (in the Izu-Bonin slab) to ~54 km (in the Kuril Islands). The seismogenic zone is nowhere more vertically broad than 40 km (measured as the difference between the shallow and deep limits). Sw varies from ~70 km (Manila slab) to ~195 km (Alaska slab), averaging about 115 km. Our estimates are ~30% larger than older estimates [e.g., (24)]. Instead of assuming a planar geometry with average subduction dip, we calculated Sw as the average down-dip distance between the upper and lower depth limits of the seismogenic zone along the nonplanar subduction zone interface. In Table 1, we also provide seismogenic zone properties for major sections within each subduction zone to better understand how seismogenesis varies along individual slabs.

When Sw is plotted versus the maximum observed earthquake magnitude in these subduction zones (fig. S9), we find a weak positive correlation. In general, the largest earthquakes occur where the seismogenic zone is wide (more than ~100 km), and narrow seismogenic zones (less than ~100 km) tend to host only small earthquakes, but notable outliers are evident. Southern Chile and Kamchatka have fairly narrow (Sw ~ 100 km) seismogenic zones yet have hosted magnitude 9+ earthquakes, whereas Java and New Guinea have extremely broad (Sw > 160 km) seismogenic zones but are not known to have hosted great-sized earthquakes. These results imply that Sw is not the singular controlling factor in potential earthquake size. Along-strike geometry (strike-parallel distance) is equally important (6), as are other seismogenic zone properties.

Slab2 is the most complete database of detailed 3D subduction zone geometries created. It includes slab geometries for the vast majority of global subduction zones and is built upon a robust and open-source methodology that should facilitate further improvements to our knowledge

of the fate of subducted slabs. There are a multitude of uses for these geometry models, from earthquake (4) and tsunami (10) hazard analyses to studies of mantle flow (11). As we have shown here, Sw does not play a dominant role in controlling the maximum size of earthquakes in subduction zones, but Slab2 provides the data necessary to better understand what geometrical control—if any—is exerted on earthquake rupture. To first order, Slab2 may also be used to identify whether segment boundaries in subduction zones are related to geometrical features on the megathrust (25), a key step in being able to assess the long-term persistence of subduction zone segmentation (26). These examples are just a few of many applications for Slab2, making it possible to better understand the interactions between slab bodies and a variety of other Earth processes.

#### REFERENCES AND NOTES

- G. P. Hayes, D. J. Wald, R. L. Johnson, *J. Geophys. Res.* **117**, B01302 (2012).
- G. P. Hayes et al., *Nature* **512**, 295–298 (2014).
- D. Melgar et al., *Geophys. Res. Lett.* **43**, 961–966 (2016).
- M. Pagani et al., *Seismol. Res. Lett.* **85**, 692–702 (2014).
- P. Audet, R. Bürgmann, *Nature* **510**, 389–392 (2014).
- Q. Bletery et al., *Science* **354**, 1027–1031 (2016).
- T. H. Dixon et al., *Proc. Natl. Acad. Sci. U.S.A.* **111**, 17039–17044 (2014).
- C. M. Eakin, M. D. Long, *J. Geophys. Res.* **118**, 4794–4813 (2013).
- G. M. Yogodzinski et al., *J. Petrol.* **56**, 441–492 (2015).
- E. Geist, P. Lynett, *Oceanography* **27**, 86–93 (2014).
- M. Morishige, S. Honda, *Earth Planet. Sci. Lett.* **365**, 132–142 (2013).
- O. Gudmundsson, M. Sambridge, *J. Geophys. Res.* **103** (B4), 7121–7136 (1998).
- E. M. Syracuse, G. A. Abers, *Geochem. Geophys. Geosyst.* **7**, Q05017 (2006).
- D. E. Portner, G. P. Hayes, *Geophys. J. Int.* **215**, 325–332 (2018).
- Materials and methods are available as supplementary materials.
- R. Hall, *Tectonophysics* **144**, 337–352 (1987).
- J. Wu, J. Suppe, R. Lu, R. Kanda, *J. Geophys. Res.* **121**, 4670–4741 (2016).
- I. D. Ripper, *Tectonophysics* **87**, 355–369 (1982).
- R. J. Holm, W. Richards, *Aust. J. Earth Sci.* **60**, 605–619 (2013).
- X. Pérez-Campos et al., *Geophys. Res. Lett.* **35**, L18303 (2008).
- D. Melgar et al., *Geophys. Res. Lett.* **45**, 2633–2641 (2018).
- A. Scire, G. Zandt, S. Beck, M. Long, L. Wagner, *Geosphere* **13**, 665–680 (2017).
- P. A. McCrory, J. L. Blair, F. Waldhauser, D. H. Oppenheimer, *J. Geophys. Res.* **117**, B09306 (2012).
- J. F. Pacheco, L. R. Sykes, C. H. Scholz, *J. Geophys. Res.* **98** (B8), 14133–14159 (1993).
- G. P. Hayes, S. M. Plescia, G. Moore, “Inferring rupture characteristics using new databases for 3D slab geometry and earthquake rupture models,” paper presented at the 2017 Fall Meeting of the American Geophysical Union, New Orleans, LA, 11 to 15 December 2017 (T23F-0663).
- A. J. Meltzner et al., *J. Geophys. Res.* **117**, B04405 (2012).
- U.S. Geological Survey, Search Earthquake Catalog; <http://earthquake.usgs.gov/earthquakes/search/>.
- E. R. Engdahl, R. D. Van Der Hilst, R. P. Buland, *Bull. Seismol. Soc. Am.* **88**, 722–743 (1998).
- G. Ekström, M. Nettles, A. M. Dziewoński, *Phys. Earth Planet. Inter.* **200–201**, 1–9 (2012).
- P. Wessel, W. H. F. Smith, *EOS Trans. Am. Geophys. Union* **72**, 441–446 (1991).
- G. P. Hayes, The Slab2 online repository, ScienceBase (2018); <https://doi.org/10.5066/F7PV6JNV>.

#### ACKNOWLEDGMENTS

We thank internal USGS reviewer W. Yeck, J. Dewey, three anonymous reviewers, and the editor for comments that helped improve the manuscript. Any use of trade, product, or firm names is for descriptive purposes only and does not imply endorsement by the U.S. Government. **Funding:** This work was funded exclusively by the U.S. Geological Survey. **Author contributions:** G.P.H. conceived of the model and wrote the paper. G.L.M., D.E.P., G.P.H., M.H., and M.F. wrote the Slab2 code base. G.P.H., G.L.M., H.F., and D.E.P. compiled data sources. G.P.H., G.M.S., and G.L.M. created figures, visualizations, and database structures.

**Competing interests:** The authors declare no competing interests.

**Data and materials availability:** Global datasets are from the Advanced National Seismic System Comprehensive Catalog (27), the EHB global relocated earthquake catalog (28), and the Global CMT catalog (29). Figures were made with the Generic Mapping Tools software package (30). Slab2 is openly available via ScienceBase (31). The Slab2 code base is available via GitHub (<https://github.com/usgs/slab2>). We welcome feedback and contributions of new slab-related datasets for future improvements of the model.

#### SUPPLEMENTARY MATERIALS

[www.sciencemag.org/content/362/6410/58/suppl/DC1](http://www.sciencemag.org/content/362/6410/58/suppl/DC1)

Supplementary Text

Figs. S1 to S9

Tables S1 to S3

References (32–42)

7 March 2018; accepted 31 July 2018

Published online 9 August 2018

10.1126/science.aat4723

## Slab2, a comprehensive subduction zone geometry model

Gavin P. Hayes, Ginevra L. Moore, Daniel E. Portner, Mike Hearne, Hanna Flamme, Maria Furtney and Gregory M. Smoczyk

Science 362 (6410), 58-61.  
DOI: 10.1126/science.aat4723 originally published online August 9, 2018

### Detailing subduction zones

Subduction zones are responsible for the most-damaging and tsunami-generating great earthquakes. Hayes *et al.* updated their Slab1.0 model to include all seismically active subduction zones, including geometrically complex regions like the Philippines. The new model, Slab2, details the geometry of 24 million square kilometers of subducted slabs, from ocean trench to upper mantle. The model will be vital for fully understanding seismic hazard in some of the most populated regions in the world.

Science, this issue p. 58

### ARTICLE TOOLS

<http://science.scienmag.org/content/362/6410/58>

### SUPPLEMENTARY MATERIALS

<http://science.scienmag.org/content/suppl/2018/08/08/science.aat4723.DC1>

### REFERENCES

This article cites 36 articles, 6 of which you can access for free  
<http://science.scienmag.org/content/362/6410/58#BIBL>

### PERMISSIONS

<http://www.scienmag.org/help/reprints-and-permissions>

Use of this article is subject to the [Terms of Service](#)

---

Science (print ISSN 0036-8075; online ISSN 1095-9203) is published by the American Association for the Advancement of Science, 1200 New York Avenue NW, Washington, DC 20005. The title *Science* is a registered trademark of AAAS.

Copyright © 2018 The Authors, some rights reserved; exclusive licensee American Association for the Advancement of Science. No claim to original U.S. Government Works